Macromolecules **1991,** *24,* 3821-3827

Chain Fragment Diffusion in Liquid and Glassy Polymer Blends

E. H. Hellmann

Max-Planck-Institut für Polymerforschung, D-6500 Mainz, Germany

G. P. Hellmann*

Deutsches Kunststoff-Institut, Schlossgartenstrasse 6, D-6100 Darmstadt, Germany

A. R. Rennie

Institut Laue-Langevin, F-38042 Grenoble, France

Received July 9, 1990; Revised Manuscript Received February 5, 1991

ABSTRACT: A new technique for measurements of extremely slow chain diffusion in polymer blends is discussed. It involves the analysis of "chain fragment diffusion by small-angle neutron scattering (CFD-SANS)". The principle is that polymer chains are split in the glassy state in a condition where the chain conformation does not immediately respond to the fragmentation. The subsequent separation of chain fragments can then be followed with SANS. In order to obtain contrast for SANS measurements, chain fragmentation of a deuterated polymer was made in a hydrogenous matrix. Experiments are described on a copolycarbonate containing a thermosensitive comonomer in a matrix of tetramethyl polycarbonate. Diffusion coefficients in the range 10^{-18}–10^{-14} cm^2/s were measured in a temperature range from 24 K below to 14 K above the glass transition. Evaluation of the data was based on a statistical analysis of the CFD process.

1. Introduction

A number of techniques have been developed over the past 10 years to measure the slow chain diffusion that occurs in bulk polymers and polymer blends.[1] Methods such as forced Rayleigh scattering,[2,3] forward recoil spectrometry,[4] and multilayer[5,6] or latex[7,8] interdiffusion monitored with small-angle neutron scattering (SANS) have permitted determination of diffusion coefficients as low as 10^{-16} cm^2/s. Diffusion on this scale is characteristic of highly viscous polymers, not much above the glass transition temperature.

The present paper deals with a new method that measures the chain fragment diffusion by SANS (CFD-SANS), which permits measurements of even smaller diffusion coefficients, even those in the glassy state. This technique has been discussed in refs 9–11. The principle is shown outlined in Figure 1. When polymer chains are split into fragments at temperatures well below the glass transition, the fragmentation (with characteristic time τ) can be much faster than the diffusion of the fragments (with correlation time δ). No immediate change in the chain conformation is associated with this fragmentation process $0 \rightarrow 0^*$ as the pieces remain arranged as in the state 0. The correlations between the fragments are only reduced gradually by the chain fragment diffusion (CFD) on the time scale δ (process $0^* \rightarrow \infty$). If a fragmentable polymer X is blended with a second polymer M, which serves as a matrix, the polymer concentration fluctuations can be observed as structure factor S_ϕ of the blend with SANS. The small spatial distances probed by SANS permit the detection of diffusion on length scales on the order of fragment coil diameters.

The polymer X has two equilibrium states. In the state 0 the chains are still intact, while in the final state ∞, the fragments are entirely uncorrelated. The chain structure factor S of the molecules in each of these states is given by[12]

$$\frac{1}{S_i} \sim \frac{1}{V_{wi}} + \frac{1}{12}C^2q^2, \quad i = 0, \infty \tag{1}$$

where V_w is the weight-average volume per chain or fragment and C is the chain stiffness parameter of the polymer X. Chains in state 0^* have the chain structure factor S_0. The chain structure factor in the final state S_∞ is different from S_0 mainly by the variation of V_w and to a lesser extent by the variation in C.

SANS actually measures the structure factor of the blend S_ϕ, which depends on S_i, the chain structure factor of the matrix polymer S_M, and the interaction parameter of the blend χ:

$$\frac{1}{S_{\phi i}} = \frac{1}{S_i} + \frac{1}{S_M} - 2\chi, \quad i = 0, \infty \tag{2}$$

During the diffusion process $0^* \rightarrow \infty$, the structure factor observed with SANS will change from $S_{\phi 0}$ to $S_{\phi\infty}$. This is discussed further below from both theoretical and experimental viewpoints.

A system suitable for such a study is the blend of a copolymer of Bisphenol A (unit CA) and the thermosensitive diol 1,1,2,2-tetraethyl-1,2-bis(p-hydroxyphenyl)ethane (unit CT)

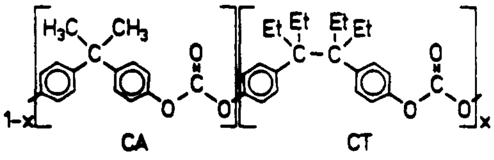

PC(T$_x$A$_{1-x}$)

with the homopolymer tetramethyl polycarbonate (TMPC).

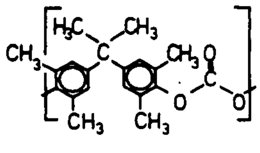

TMPC

The blends of PC(T$_x$A$_{1-x}$) and TMPC are homogeneous.[10,14]

The synthesis and thermal fragmentation of the copolymer have been described previously.[11,15] The central

---

* To whom all correspondence should be sent.

0024-9297/91/2224-3821$02.50/0

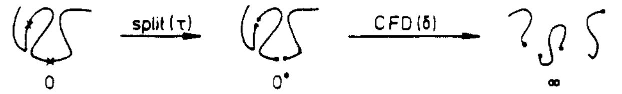

Figure 1. Chain fragmentation ($0 \rightarrow 0^*$, reaction time constant τ) and subsequent chain fragment diffusion ($0^* \rightarrow \infty$, CFD correlation time δ). State 0^* is only formed when $\tau \ll \delta$.

C–C bond of the CT unit splits in a first-order thermally activated reaction ending in radical disproportionation.

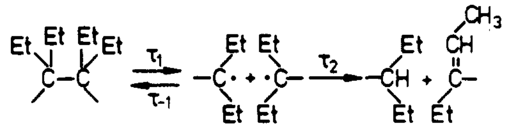

$$\tau = \tau_1(1 + \tau_2/\tau_{-1}) = \tau^* \exp\left(\frac{E^*}{R}\right)\left(\frac{1}{T} - \frac{1}{T^*}\right), \quad \tau^* = 1\ \mathrm{h} \tag{3}$$

The time constant τ for the reaction is governed by the activation energy $E^* = 176$ kJ/mol and the characteristic temperature $T^* = T(\tau^*) = 172$ °C.[11] Fragmentation has been shown to proceed at the same rate in the pure copolymers and in their blends with TMPC in both liquid and glassy states.

There are three conditions that a blend should satisfy to perform adequately in such experiments:

(1) There must be a sufficiently large difference between S_0 and S_∞. From eq 1 it is seen that this implies a large difference between V_{w0} and $V_{w\infty}$. It turns out that $x \geq 0.1$ is required for good kinetic studies.

(2) The glass transition temperature of the blend given by (ϕ = volume fraction of copolymer)

$$\frac{1}{T_g} = \frac{\phi}{T_{gi}} + \frac{1-\phi}{T_{gM}}, \quad i = 0, \infty \tag{4}$$

$$T_{g\infty} = T_{g0} - \frac{2k}{V_{w\infty}}, \quad k = 120\ \mathrm{K\ nm^3} \tag{5}$$

must be higher than the characteristic temperature T^*. Equation 5 shows that T_g is different in the states 0 and ∞[10,11,16,17] ($T_{g0} = 150$ °C, $T_{gM} = 202$ °C). The blend in state 0* will already have the final glass transition temperature, and so our condition is that $T_{g\infty} > T^*$. In practice this imposes limits on $x < 0.2$ and $\phi < 0.2$.

(3) The copolymer content ϕ in the blend must be sufficiently large to give adequate neutron-scattering contrast.

The blend of PC(T_xA_{1-x})/TMPC (from now on denoted as X/M) chosen for this study had $x = 0.16$ and $\phi = 0.12$. This gives sufficient contrast and an optimal balance of a large ratio $V_{w0}/V_{w\infty} \cong 10$ and a high glass transition temperature $T_g = 186$ °C. CFD–SANS experiments were carried out close to the glass transition in the range 162–200 °C, i.e., from 24 K below to 14 K above T_g. (In this paper the glass transition temperature T_g always refers to measurements by DSC at 20 K/min.)

At temperatures near or above T_g the diffusion is always faster than chain fragmentation. In order to obtain the state 0*, it was necessary to prefragment the copolymers by annealing at 150 °C, i.e., at $T_g - 36$ K. At lower temperatures prefragmentation proved unnecessary as state 0* was formed sufficiently fast in comparison to the diffusion process.

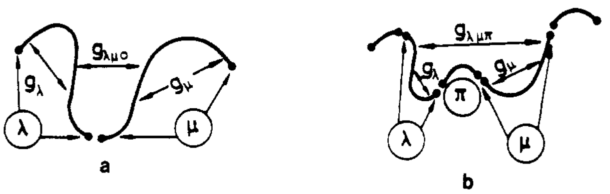

Figure 2. (a) Correlation functions in a two-block polymer, with blocks λ and μ. (b) Correlation functions in a multiblock polymer, with two blocks separated by a monomer sequence π. Debye functions g_λ and g_μ (eq 10), cross-correlation functions $g_{\lambda\mu0}$ (eq 13) and $g_{\lambda\mu\pi}$ (eq 20).

2. Theory of CFD

The structure factor of a blend X/M

$$S_\phi(\mathbf{q}) = V_{\mathrm{total}}\langle\delta\phi(\mathbf{q})^2\rangle \tag{6}$$

is in the mean-field approximation[13] given by eq 2. In eq 6 V_{total} is the total volume and $\delta\phi$ is a fluctuation in the volume fraction ϕ of polymer X with wave vector $\mathbf{q}$. The symbol $\langle\ \rangle$ denotes a configurational average. The structure factors S_0 and S_∞ of the polymer X in the states 0 and ∞ are given by

$$S_0(\mathbf{q}) = \frac{v^{*2}}{V_{\mathrm{total}}}\sum_\nu\Big(\sum_{\alpha\beta\epsilon\nu} e^{-\langle r_{\alpha\beta}^2\rangle \mathbf{q}^2/6}\Big)N_\nu \tag{7a}$$

$$S_\infty(\mathbf{q}) = \frac{v^{*2}}{V_{\mathrm{total}}}\sum_\lambda\Big(\sum_{\alpha\beta\epsilon\lambda} e^{-\langle r_{\alpha\beta}^2\rangle \mathbf{q}^2/6}\Big)N_\lambda \tag{7b}$$

where v^* is the volume per monomer. In eq 7a $r_{\alpha\beta}$ is the separation of two monomers α and β in the same chain of degree of polymerization ν ($\alpha\beta\epsilon\nu$). Equation 7b is of identical form but refers to the fragment with a degree of polymerization λ. If the index M were to be substituted, eq 7a would also hold for S_M, the structure factor of the matrix polymer M.

Under the conditions of the mean-field approximation two monomers on the same chain or fragment will have a mean-square separation[13] given by

$$\langle r_{\alpha\beta}^2\rangle = 6|\alpha - \beta|L^2 \tag{8}$$

where $|\alpha - \beta|$ is the separation in numbers of monomers and $L^2 = R_\nu^2/\nu = R_\lambda^2/\lambda$ is the reduced radius of gyration. This amounts to an assumption of Gaussian chain statistics for both the chains and the fragments.

Next the structure factors S_0 and S_∞ and the transition $0^* \rightarrow \infty$ (Figure 1) due to CFD are discussed. First the case of a monodisperse polymer with two monodisperse fragments is considered before the case of a polydisperse polymer with several polydisperse fragments is discussed.

2.1. Monodisperse Diblock Polymers X.

The degree of polymerization for the initial polymer is ν, and it splits into two fragments of size λ and μ such that $\nu = \lambda + \mu$ as illustrated in Figure 2a. The structure factors of the states 0* and ∞ are

$$S_0 = \phi v^* \nu g_\nu \tag{9a}$$

$$S_\infty = \phi v^* \frac{\lambda^2 g_\lambda + \mu^2 g_\mu}{\lambda + \mu} \tag{9b}$$

where the structure factor of the chains and fragments can be described by the Debye function

$$g_i = \frac{1}{i^2}\sum_{\alpha\beta\epsilon i} Q^{|\alpha-\beta|} = \frac{1}{i(1-Q)}\left(1 + Q - 2Q\frac{1-Q^i}{i(1-Q)}\right), \quad i = \nu, \lambda, \mu \quad (10)$$

where the notation $Q = e^{-L^2q^2}$ was used. This is often approximated as

$$g_i = \frac{2}{iL^2q^2}\left(1 - \frac{1-Q^i}{iL^2q^2}\right), \quad i = \nu, \lambda, \mu \quad (11)$$

The function S_0 contains information on correlations between monomers $\alpha\epsilon\lambda$ and $\beta\epsilon\mu$, which belong to the same chain but not the same fragment. These correlations are absent in S_∞. The difference can be expressed as follows:

$$S_0 - S_\infty = 2\phi\upsilon^*\frac{\lambda\mu}{\lambda+\mu}g_{\lambda\mu0} \quad (12)$$

with

$$g_{\lambda\mu0} = \frac{1}{\lambda\mu}\sum_{\substack{\alpha\epsilon\lambda\\ \beta\epsilon\mu}} Q^{|\alpha-\beta|} = \frac{Q}{\lambda\mu}\,\frac{(1-Q^\lambda)(1-Q^\mu)}{(1-Q)^2} \quad (13)$$

While the Debye functions g_λ and g_μ describe the intrafragment correlations, the function $g_{\lambda\mu0}$ describes the interfragment correlations. The subscript 0 is attached to $g_{\lambda\mu0}$ to indicate that the fragments λ and μ are direct neighbors in the chains.

The correlations expressed by $g_{\lambda\mu0}$ will disappear during CFD, and eq 8 for the separation of two monomers α and β on different fragments λ and μ becomes

$$\langle r_{\alpha\beta}{}^2\rangle = 6|\alpha-\beta|L^2 + 6(D_\lambda + D_\mu)t \quad (14)$$

where D_λ and D_μ are the self-diffusion coefficients of the two fragments. This expression assumes that CFD proceeds only by the random-walk motion of the centers of gravity of the two fragments. A condition is that the intrinsic relaxation modes of the fragments have relaxed by the time t. The changes in structure factor due to CFD can then be expressed as

$$S(t) = S_\infty + 2\phi\upsilon^*\frac{\lambda\mu}{\lambda+\mu}g_{\lambda\mu0}e^{-(D_\lambda+D_\mu)q^2t} \quad (15)$$

or

$$S(t) = S_\infty + (S_0 - S_\infty)e^{-(D_\lambda+D_\mu)q^2t} \quad (16)$$

or using the diffusion time constant δ as introduced in Figure 1:

$$S(t) = S_\infty + (S_0 - S_\infty)e^{-t/\delta} \quad (17)$$

2.2. Polydisperse Multiblock Polymers. Both the chains and fragments have a distribution in length. The number of fragments per chain will also vary. The structure factors S_0 before and S_∞ after CFD are given by modifications of eq 9 (Figure 2b)

$$S_0 = \phi\upsilon^*\frac{\langle\nu^2g_\nu\rangle_{\rm n}}{\langle\nu\rangle_{\rm n}} = \phi\upsilon^*\langle\nu g_\nu\rangle_{\rm w} \quad (18a)$$

$$S_\infty = \phi\upsilon^*\frac{\langle\lambda^2g_\lambda\rangle_{\rm n}}{\langle\lambda\rangle_{\rm n}} = \phi\upsilon^*\langle\lambda g_\lambda\rangle_{\rm w} \quad (18b)$$

where $\langle\ \rangle_{\rm n}$ denotes a number average and $\langle\ \rangle_{\rm w}$ denotes a weight average. The polydisperse version of eq 12 is in general

$$S_0 - S_\infty = 2\frac{\upsilon^{*2}}{V_{\rm total}}\sum_{\lambda\mu\pi}\Big(\sum_{\substack{\alpha\epsilon\lambda\\ \beta\epsilon\mu}} Q^{\pi+|\alpha-\beta|}\Big)N_{\lambda\mu\pi} \quad (19)$$

which again describes all interfragment correlations lost during the course of CFD.

The expression in eq 19 can be rather complex. Fragments λ and μ are not in general direct neighbors as was the case for the diblock polymers. The correlation function of the segments $g_{\lambda\mu\pi}$ is related to $g_{\lambda\mu0}$ (eq 13) by

$$g_{\lambda\mu\pi} = \frac{1}{\lambda\mu}\sum_{\substack{\alpha\epsilon\lambda\\ \beta\epsilon\mu}} Q^{\pi+|\alpha-\beta|} = Q^\pi g_{\lambda\mu0} \quad (20)$$

This expression is weighted in eq 9 by the number of fragments $N_{\lambda\mu\pi}$ of length λ and μ in a monomer separation π. This depends on both the chain and fragment length distributions and may be difficult to calculate. However, for ideal polycondensates it can be factorized into $N_{\lambda\mu\pi} = p_\lambda p_\mu N_\pi$ where N_π is the number the subchains (made of one or more fragments) of degree of polymerization π between fragments of arbitrary length λ and μ. In ideal polycondensates the distrributions of chains and fragments are[19]

$$p_\nu = u_0{}^{\nu-1}(1-u_0), \quad w_\nu = \nu u_0{}^{\nu-1}(1-u_0)^2$$

$$p_i = u_\infty{}^{i-1}(1-u_\infty), \quad w_i = iu_\infty{}^{i-1}(1-u_\infty)^2, \quad i = \lambda, \mu \quad (21)$$

where u_0 and u_∞ are the degrees of conversion for the intact chains and the final fragments.

This yields for eq 18

$$S_i = \frac{\phi\upsilon^*}{1-Q}\left(1 + Q - 2Q\frac{1-u_i}{1-u_iQ}\right), \quad i = 0, \infty \quad (22)$$

Expansion leads to the Zimm equation (eq 1)

$$\frac{1}{S_i} = \frac{1}{\phi}\left(\frac{1}{V_{{\rm w}i}} + \frac{1}{12}C^2q^2\right), \quad i = 0, \infty \quad (23)$$

with the volume per chain $V_{{\rm w}i} = \upsilon^*\langle i\rangle_{\rm w}$ and the square chain stiffness parameter $C_i^2 = 6L_i^2/\upsilon^*$. With the index M and exchange $\phi \rightarrow (1-\phi)$ eq 23 holds also for $S_{\rm M}$ of the matrix polymer, if it is a polycondensate.

Equation 19 reads with eqs 20 and 21

$$S_0 - S_\infty = 2\frac{\upsilon^{*2}}{V_{\rm total}}\Big(\sum_\pi Q^\pi N_\pi\Big)\langle\langle\lambda\mu g_{\lambda\mu0}\rangle\rangle_{\rm n} \quad (24)$$

with

$$\frac{\upsilon^{*2}}{V_{\rm total}}\sum_\pi Q^\pi N_\pi = \phi\upsilon^*(u_0 - u_\infty)\frac{1-u_\infty Q}{1-u_0Q} \quad (25a)$$

$$\langle\langle\lambda\mu g_{\lambda\mu0}\rangle\rangle_{\rm n} = Q\langle f_\lambda\rangle_{\rm n}{}^2, \quad f = \frac{1}{\lambda}\,\frac{1-Q^\lambda}{1-Q} \quad (25b)$$

The structure factor $S(t)$ of multiblock polymers during CFD is then, analogously to eq 15 for diblock polymers, given by

$$S(t) = S_\infty + (S_0 - S_\infty)\langle e^{-D_\lambda q^2t}\rangle_F{}^2, \quad F = \frac{f_\lambda p_\lambda}{\sum \lambda f_\lambda p_\lambda} \quad (26)$$

In the limit $q^2 < 1/(\lambda L^2)$ this can be written as

$$S(t) = S_\infty + (S_0 - S_\infty)\langle e^{-D_\lambda q^2t}\rangle_{\rm w}{}^2 \quad (27)$$

This is surprisingly simple and very similar to eq 16.

Table I
Polymers of the Blend X/M

polymer	ρ, g/cm^3	M_w	M_w/M_n	V_w, nm^3	T_g, °C
PC($T_{0.16}A_{0.84}$)D, "X"					
state 0	1.28	31 200	2.0	40.5	151
state ∞	1.21	2 850	1.7	3.9	97
TMPC, "M"	1.08	23 600	2.1	36.3	202

3. Experimental Section

Polymers and Blends. The copolycarbonate (X) PC($T_{0.16}A_{0.84}$) was prepared by the method described in ref 15 from deuterated Bisphenol A and the diol 1,1,2,2-tetraethyl-1,2-bis(*p*-hydroxyphenyl)ethane. The matrix (M) polymer TMPC was obtained from Bayer AG. Both polymers were precipitated as fine powders from methanol. Fully fragmented samples were prepared by annealing for 20 min at 200 °C. Some analytical data on these materials are listed in Table I. Densities were measured by a bouyancy technique. Molecular weights were determined by GPC with a Bisphenol A polycarbonate calibration. The chain volume is calculated as $V_w = M_w/(\rho N_A)$ where N_A is Avogadro's number. Glass transition temperatures were measured by DSC at a heating rate of 20 K/min.

Films for the SANS measurements were prepared by casting from CH_2Cl_2 and dried at 100 °C.[14] Each film was about 100 μm thick and amorphous as seen by X-rays and clear. The blend X/M ($x = 0.16$, $\phi = 0.12$) had glass transitions $T_{g0} = 197$ °C and $T_{g\infty} = 186$ °C.

CFD-SANS. The SANS experiments were carried out with the spectrometers D11 (neutron wavelength 8 Å, sample-detector distance 5 m) and D17 (12 Å, 2.8 m) at the Institut Laue-Langevin (Grenoble, France). The samples were packs of films about 1 mm thick cut to fit tightly into sample holders with thin niobium windows. The procedure for CFD-SANS measurements depended on the temperature and can be divided into two regimes.

177–200 °C: Diffusion is fast at these temperatures, and CFD was monitored on-line in the neutron beam, using only one sample per temperature. An oven consisting of a large metal block with openings for the beam was preheated to the desired temperature. A sample could be inserted rapidly, and thermal equilibrium was reached in about 1 min. The condition for establishing the state 0* ($\tau \ll \delta$, Figure 1) is not satisfied at these temperatures, and the samples were correspondingly prefragmented at 150 °C for 40 h.

162–169 °C: In this temperature range diffusion is so slow that the CFD-SANS experiments take many hours. Several samples per temperature were therefore prepared and annealed off-line for different times. They were then quenched to room temperature for subsequent SANS measurements. Prefragmentation is practically unnecessary at these temperatures as the state 0* is established in the early stages of annealing. However, as a test one set of samples was prefragmented for 40 h at 150 °C. It should be noted that quenching to room temperature may cause problems. The interaction parameter $\chi(T)$ of the blend may change, which will alter the structure factor.[20] It will be seen later that this effect is small for the blend X/M.

The SANS data evaluation and correction has been described in ref 14 and calculations of the blend structure factor S_ϕ from the normalized SANS intensities in ref 11.

4. CFD-SANS Experiments

SANS data measured during chain fragmentation at 160 °C in blends of PC(T_xA_{1-x}) with a matrix of polycarbonate (PCA) rather than TMPC have been presented in ref 11. Figure 3 shows the Zimm diagram of the strructure factor $S_\phi(t)$ of a blend PC(T_xA_{1-x})/PCA that is equal to that used in the present study in both x and ϕ. The blend had, however, a low glass transition temperature T_g = 135 °C and was fragmented at 180 °C = T_g + 55 K. The blend had under these conditions a low viscosity. Diffusion was so rapid that the measured structure factor $S_\phi(t)$ responded immediately to the fragmentation reaction ($\tau \gg \delta$). SANS provided therefore a measure of the fragmentation time constant τ rather than the CFD process.

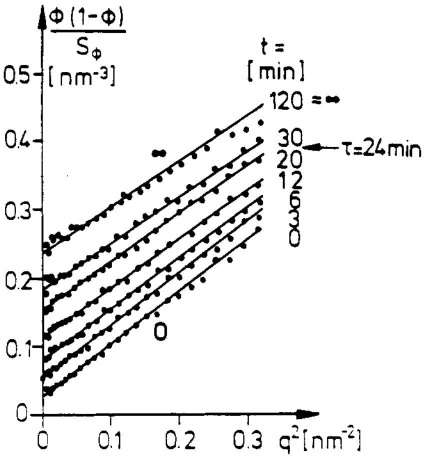

Figure 3. Zimm diagram for chain fragmentation in the blend PC($T_{0.16}A_{0.84}$)/PCA at 180 °C. τ is the time constant of eq 3.

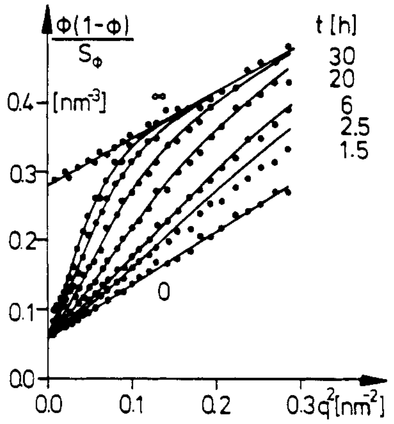

Figure 4. Zimm diagrams for chain fragmentation and subsequent CFD in the blend X/M at 162 °C. Curves were calculated with eqs 28 and 33.

The blend structure factor is given by (eq 2)

$$\frac{1}{S_\phi(t)} = \frac{1}{S(t)} + \frac{1}{S_M} - 2\chi \tag{28}$$

with $\chi = 0$ since the matrix is PCA. Thus

$$\frac{1}{S(t)} = \frac{1}{S_\infty} + \left(\frac{1}{S_0} - \frac{1}{S_\infty}\right)e^{-t/\tau} \tag{29}$$

The Zimm diagram in Figure 3 does indeed show a set of nearly parallel lines.

The Zimm diagram in Figure 4 shows that the changes in $S_\phi(t)$ are very different when the CFD process is dominant. The figure shows the CFD-SANS experiment on the blend X/M at 162 °C corresponding to T_g – 24 K. Now fragmentation occurs in an immobilized matrix ($\tau \ll \delta$), and the state 0* is established at an early stage. The changes in $S_\phi(t)$ are a response to diffusion rather than fragmentation.

Figure 5a shows a Zimm diagram for CFD in the blend X/M at 177 °C = T_g – 9 K. The blend had been prefragmented at 150 °C to establish the state 0*. The patterns in Figures 4 and 5a are clearly very similar. $S_\phi(t)$ is seen to change slowly at low q and faster at high q, which is typical of a diffusion process. The diffusion is always slower at larger length scales. Figure 5b demonstrates that CFD could be monitored to the very late stages.

A momentum transfer range of $0.06 < q < 0.6$ nm^{-1} was used for the SANS measurements. The diffusion distances probed are thus of the order of a few times the radius of gyration of the fragments. Data were evaluated by using

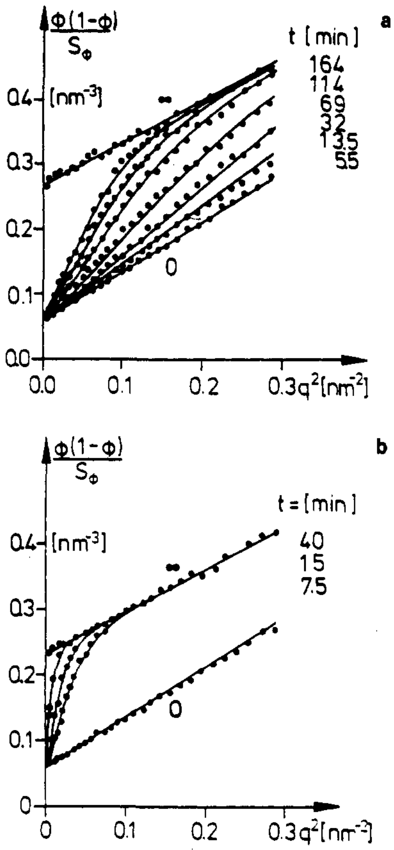

Figure 5. Zimm diagram for CFD in the prefragmented blend X/M at (a) 177 °C and (b) 190 °C. Curves were calculated with eqs 28 and 33.

eq 28 together with eq 27. The Zimm curves for state 0* and state ∞ are described by eqs 23 and 28 with the chain and fragment volumes listed in Table I. The chain stiffness parameters are $C_0^2 = C_M^2 = 9.5$ nm^{-1} and $C_\infty^2 = 8.0$ nm^{-1}, and $\chi = -0.15$ nm^{-3} is the interaction parameter.[11,14]

The diffusion coefficient D_λ in eq 27 was assumed to be of the form

$$D_\lambda(T) = D_1(T)\,\lambda^{-\alpha} \tag{30}$$

where D_1 is the temperature-dependent prefactor and α is the exponent describing the variation of diffusion rate with chain length. For Rouse diffusion $\alpha = 1$ and for reptation $\alpha = 2$ is expected.[13] In the liquid state, the temperature dependence of D_1 will be given approximately by the universal WLF equation[21]

$$D_1(T) \sim \exp\frac{C_1(T-T_g)}{C_2 + (T-T_g)},\quad C_1 = 17.4,\ C_2 = 51.6\ \mathrm{K} \tag{31}$$

A difficulty with eq 30 is that D_1 describes the diffusion of monomers. This is not well reflected in the data. It is more useful to replace the equation with

$$D_\lambda(T) = D_{w\infty}(T)\left(\frac{\lambda}{\langle\lambda\rangle_w}\right)^{-\alpha} \tag{32}$$

where $D_{w\infty}$ describes the diffusion of a fragment with the weight-average degree of polymerization $\langle\lambda\rangle_w = 10.7$ (equivalent to $V_{w\infty} = 3.9$ nm^3).

Figure 6 shows the time decay function (eq 27 and 32):

$$\Psi(x) = \frac{S(t) - S_\infty}{S_0 - S_\infty} = \left\langle \exp\left(\frac{\lambda}{\langle\lambda\rangle_w}\right)^{-\alpha} q^2 x\right\rangle_w,\quad x = D_{w\infty}t \tag{33}$$

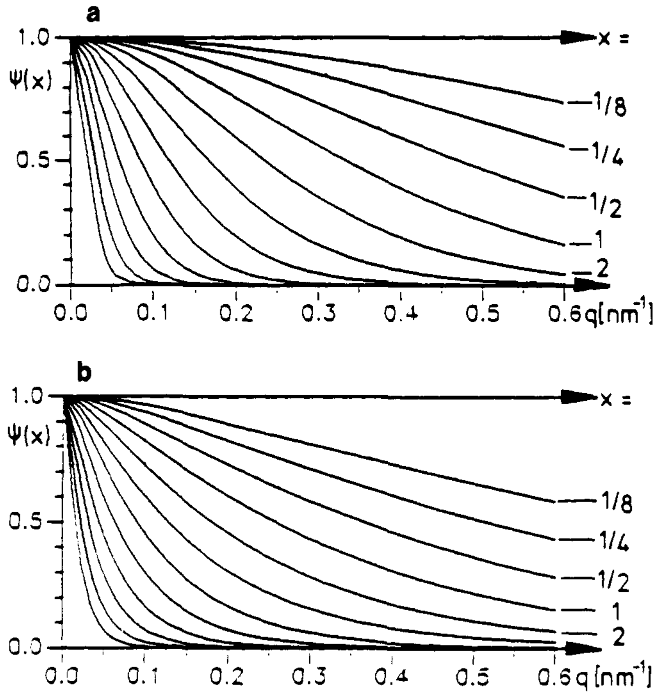

Figure 6. Time decay function $\Psi(x)$ of eq 33 at different reduced times x with (a) $\alpha = 1$ and (b) $\alpha = 2$.

The curves are plotted for $\alpha = 1$ and $\alpha = 2$ for various reduced times x. Figure 7 presents the corresponding Zimm diagrams (eq 28). The similarity with Figures 4 and 5 is obvious.

The curves for $\alpha = 1$ and $\alpha = 2$ are of a very similar character, so that there is no chance to determine α reliably. The volume per fragment $V_{w\infty}$ of the copolymer X corresponds to the entanglement limit of PCA.[22] Nevertheless, $\alpha = 1$ for Rouse diffusion was assumed, which leaves $D_{w\infty}$ as the only fit parameter in eq 33. Zimm diagrams of the CFD process were fitted with eqs 28 and 33. The first curve in time lagged usually behind but the description was generally satisfactory (Figures 4 and 5).

Diffusion coefficients $D_{w\infty}$ are shown in Figure 8. They cover the extremely low range $10^{-18} < D_{w\infty} < 10^{-14}$ cm^2/s. CFD at 200 °C was already too fast to measure, while it took weeks to arrive at state ∞ at 162 °C.

The "WLF" line results from eq 31, assuming that the WLF law holds for $T \geq 200$ °C. Comparison with the experimental $D_{w\infty}$ data shows that these change markedly less with temperature. This agrees with results from dynamic relaxation spectroscopy on glassy polymers.[23] Segmental relaxation and as now shown by Figure 8 also chain diffusion is in glassy polymers faster than predicted. The WLF law describes the mobility in equilibrium, but glassy polymers have an enhanced mobility, due to extra free volume.

Annealing the blend X/M below T_g was expected to decrease free volume and mobility. Indeed this effect is seen in Figure 8. CFD was measured at 166 °C with prefragmented as well as not prefragmented samples. The former, but not the latter, sample has received an annealing period of 40 h at 150 °C. Figure 8 shows that $D_{w\infty}$ is considerably lower for the pretreated samples.

5. Discussion

This study shows that measuring CFD in blends with SANS is a good technique for the investigation of slow chain diffusion on a scale that is almost molecular. Extremely slow diffusion can be studied, even in the glassy state, because of the very high spatial resolution of SANS.

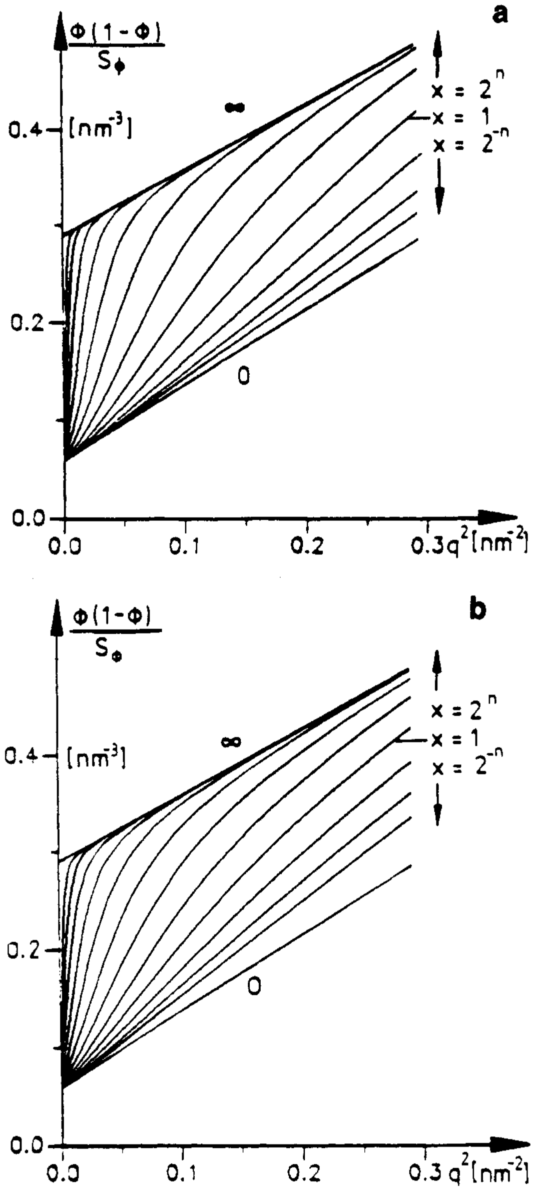

Figure 7. Zimm diagrams corresponding to Figure 6, calculated with eqs 28 and 33 with (a) $\alpha = 1$ and (b) $\alpha = 2$.

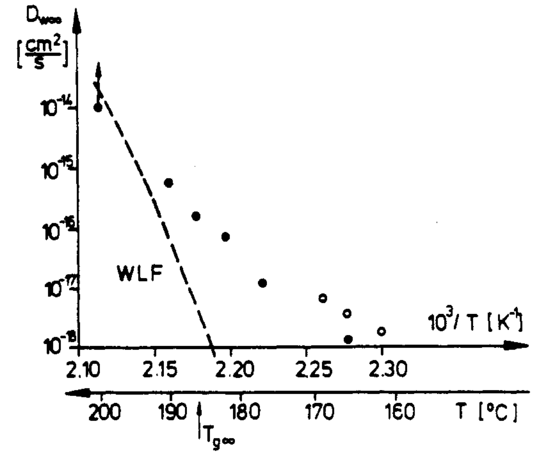

Figure 8. Arrhenius diagram for the diffusion coefficient $D_{w\infty}$ of CFD in the blend X/M: (●) prefragmented, (○) not prefragmented. Line "WLF" was calculated with eq 31.

In principle, any process can be used to measure such low diffusion coefficients given the following conditions:

(a) An equilibrium state is approached from an initial well-defined nonequilibrium state.

(b) There is sufficient difference between the initial and final structure factors.

(c) Diffusion occurs in the spatial scale accessible to SANS.

The most straightforward experiment is the temperature jump technique in which diffusion is measured in blends after a sudden change in temperature, which modifies the interaction parameter χ.[24,25]

It is informative to compare this with CFD-SANS. A temperature jump experiment could be made with the blend X/M as follows. First the copolymer X is entirely fragmented. A blend film is then cast at room temperature. The structure factor $S_{\phi I}$ of this film is given by eq 2 with $\chi_I = -0.19\ \mathrm{nm}^{-3}$. After a jump into the temperature range 160–200 °C the structure factor will be $S_{\phi II}$ with $\chi_{II} = -0.15\ \mathrm{nm}^{-3}$ (ref 14). At intermediate times the structure factor will change according to[24,25]

$$S_\phi(t) = S_{\phi II} + (S_{\phi I} - S_{\phi II})e^{-t/\delta} \tag{34}$$

This assumes that X and M are monodisperse.

The small chain length and low glass transition temperature of the fragments of X make the "fast mode" model for polymer interdiffusion[26,27] appropriate. This gives an expression for the time constant δ in eq 34

$$\frac{1}{\delta} = 2D_{\mathrm{inter}}q^2 = 2\frac{\phi(1-\phi)}{S_{\phi II}}((1-\phi)V_X D_X + \phi V_M D_M)q^2 \cong 2D_X q^2 \tag{35}$$

where D_{inter} is the interdiffusion coefficient of the blend and D_X and D_M are the self-diffusion coefficients of the components. The expectation is that the more mobile fragments of X diffuse relatively rapidly and swell the matrix M, which may be considered as a passive network. The time constant δ depends then only on the diffusion of the fragments of X.

The expression for δ in eq 35 corresponds to that in eq 17 for CFD in blends with a diblock polymer. In the approximation

$$\frac{1}{\delta} = 2D_{w\infty}q^2 \tag{36}$$

which is quite good, even the expression for polydisperse multiblock polymers (eq 27) appears the same as eq 34. There are, however, two important points to consider:

(1) The temperature jump technique, simple and attractive as it is, suffers from a lack of generality in its applicability. The total effect to be measured is $S_{\phi I} - S_{\phi II}$, which is governed by the temperature dependence of the interaction parameter χ:

$$\frac{1}{S_{\phi I}} - \frac{1}{S_{\phi II}} = -2(\chi_I - \chi_{II}) \tag{37}$$

Often this effect is insufficiently large. In the case of the blend X/M, it is immeasurably small. It is also difficult to predict $\chi(T)$. An advantage of the CFD-SANS experiment is that the measured effect $S_0 - S_\infty$ is governed by the chain and fragment lengths, which can be adjusted as required:

$$\frac{1}{S_0} - \frac{1}{S_\infty} \approx \frac{1}{\phi}\left(\frac{1}{V_{w0}} - \frac{1}{V_{w\infty}}\right) \tag{38}$$

It is clear that it is advantageous to work with multiblock polymers. For a diblock polymer $S_0 - S_\infty$ is not so large since $V_0 = 2V_\infty$ (for equal blocks).

(2) An attractive feature of the CFD-SANS technique is that it is possible to construct a detailed theoretical model. A description in terms of single-chain diffusion is straightforward. It is not so simple to incorporate the effects on diffusion of interactions between the polymer X and the matrix polymer M during CFD. No attempt

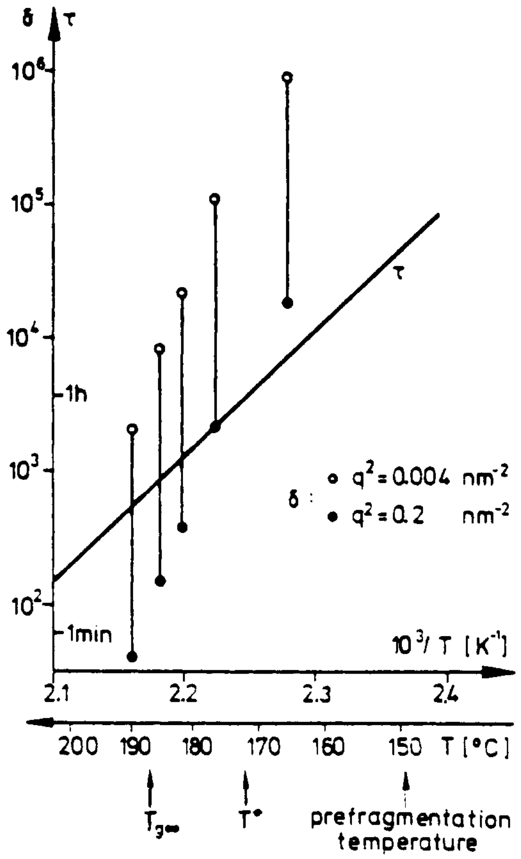

Figure 9. Arrhenius diagram for τ (eq 3) and δ (eq 36). Bars indicate the range of δ covered by the q scale of SANS.

has yet been made to include such effects, and the kinetic processes are expressed only in terms of the static blend structure factors. Investigation of a better description is in progress.

A final remark concerns the crucial condition on which CFD-SANS measurements are based, i.e., the change from $\tau \gg \delta$ to $\tau \ll \delta$ in the region of the glass transition. The variation of τ as given by eq 3 and δ as approximated by eq 36 is plotted in Figure 9. The values of q^2 indicate the limits of the range covered by SANS in these experiments. The temperature range $\tau \ll \delta$ in which a well-defined state 0* is formed is seen to begin below $T \cong T^* = 172$ °C.

Acknowledgment. Financial support from the Bundesminister für Forschung und Technologie is gratefully acknowledged.

References and Notes

(1) Binder, K.; Sillescu, H. Polymer–Polymer Diffusion. *Encyclopedia of Polymer Science and Engineering*, 3rd ed.; Wiley-Interscience Publishers: New York, 1991.
(2) Leger, L.; Hervet, H.; Rondelez, F. *Macromolecules* **1981**, *14*, 1732.
(3) Antonietti, M.; Coutandin, J.; Grütter, R.; Sillescu, H. *Macromolecules* **1984**, *17*, 798.
(4) Green, P. F.; Mills, P. J.; Palmstrom, C. J.; Mayer, J. W.; Kramer, E. J. *Phys. Rev. Lett.* **1984**, *53*, 2145.
(5) Bartels, C. R.; Graessley, W. W.; Crist, B. *J. Polym. Sci., Polym. Lett. Ed.* **1983**, *21*, 495.
(6) Stamm, M. *Polym. Prepr. (Am. Chem. Soc., Div. Polym. Chem.)* **1987**, *28* (2), 56.
(7) Hahn, K.; Ley, G.; Schuller, H.; Oberthür, R. *Colloid Polym. Sci.* **1986**, *264*, 1092.
(8) Anderson, J. E.; Jou, J. H. *Macromolecules* **1987**, *20*, 1544.
(9) Meurer, E.; Hellmann, G. P.; Rennie, A. R. In Chain Molecule Diffusion in Glasses. *Polymer Motion in Dense Systems*; Richter, D., Springer, T., Eds.; Springer Verlag: Berlin, 1988; p 98.
(10) Meurer, E.; Kuhn, K. J.; Hellmann, G. P.; Rennie, A. R. *J. Polym. Sci., Polym. Phys. Ed.* **1990**, *28*, 893.
(11) Hellmann, E. H.; Kuhn, K. J.; Hellmann, G. P.; Rennie, A. R.; *J. Polym. Sci., Polym. Phys. Ed.*, in press.
(12) Benoit, H. *J. Polym. Sci.* **1953**, *11*, 507.
(13) de Gennes, P.-G. *Scaling Concepts in Polymer Physics*; Cornell University Press: Ithaca, NY, 1979.
(14) Hellmann, E. H.; Hellmann, G. P.; Rennie, A. R. *Colloid Polym. Sci.* **1991**, *269*, 343.
(15) Kuhn, K. J.; Hellmann, G. P. *J. Polym. Sci., Polym. Phys. Ed.* **1990**, *28*, 2165.
(16) Fox, T. G. *Bull. Am. Chem. Soc.* **1956**, *1*, 123.
(17) Fox, T. G.; Flory, P. J. *J. Appl. Phys.* **1950**, *21*, 581.
(18) Crank, J. *The Mathematics of Diffusion*; Clarendon Press: Oxford, 1975.
(19) Flory, P. J. *Principles of Polymer Chemistry*; Cornell University Press: Ithaca, NY, 1953; Chapter 8.1.
(20) Kramer, E. J.; Sillescu, H. *Macromolecules* **1989**, *22*, 414.
(21) Ferry, J. D. *Viscoelastic Properties of Polymers*, 3rd ed.; Wiley: New York, 1980; Chapter 11.
(22) van Krevelen, D. W.; Hoftyzer, P. J. *Properties of Polymers*, 2nd ed.; Elsevier: Amsterdam, The Netherlands, 1976; Table 15.3.
(23) Struik, L. C. E. *Physical Ageing in Amorphous Polymers and Other Materials*; Elsevier: Amsterdam, The Netherlands, 1978; Chapter 4.10.
(24) Binder, K. J. *Chem. Phys.* **1983**, *79*, 6387.
(25) Strobl, G. R. *Macromolecules* **1985**, *18*, 558.
(26) Kramer, E. J.; Green, P. F.; Palmstrom, J. *Polymer* **1984**, *25*, 473.
(27) Sillescu, H. *Makromol. Chem., Rapid Commun.* **1984**, *5*, 519; 1987, *8*, 393.

Registry No. TMPC (homopolymer), 52684-16-9; TMPC (SRU), 38797-88-5; (Bisphenol A)(carbonic acid)(1,1,2,2-tetraethyl-1,2-bis(*p*-hydroxyphenyl)ethane) (copolymer), 110783-83-0.